

Control of 400 Watt Belt-Drive and 400 Watt Ball-Screw Servo Systems Using Discrete-Time Variable Structure Control

Wook Bahn*, Sang-Hoon Lee**, Sang-Sub Lee** and Dong-II “Dan” Cho*

* ASRI/ISRC, Dept. of Electrical and Computer Engineering,
Seoul National University, Seoul, Korea. (e-mail: dicho@snu.ac.kr)

** RS Automation Co., Ltd., 38 Jinwisandan-ro, Jinwi-myeon,
Pyeongtaek-si, Gyeonggi-do, Korea

Abstract: This paper develops a discrete-time variable structure control method for servo drives. The objective is to achieve tuningless control in industrial servo systems. The developed control method is experimentally evaluated for load variations and parameter uncertainties. Experiments are performed on typical automation applications: a 400 W servo motor with a belt-drive connection and a 400 W servo motor with a ball-screw connection. The experimental results show that the developed discrete-time variable structure controller provides better performance characteristics than the conventional commercial servo controller.

1. INTRODUCTION

Most commonly, a PID-based control scheme with three cascaded closed control loops are used in servo drives (Leonhard, W, 2001). Although the basic PID controller has a simple structure, the cascaded controller is much more complex. In addition, in typical control applications, there are many additional blocks such as feedforward controllers, gain scheduling blocks, saturation blocks, low-pass or notch filters, and disturbance observers. Each control blocks has their own control parameters, which should be determined by an experienced user. As a result, tuning a PID-based servo drive, i.e., adjusting the parameters of the PID controller and all the additional functions, is usually a very time-consuming and arduous process.

The variable structure control (VSC) method has been developed to guarantee the stability and robustness against parametric uncertainties and external disturbances with matched conditions. Using the VSC method, a control system can be designed to operate with varying load conditions. However, a discrete-time implementation is required, and it is well known that the desirable properties of stability and robustness may not be achieved in discrete time (Hung, Gao, and Hung, 1993), (Gao, Wang, and Homaifa, 1995). Many theoretical approaches have been proposed to guarantee the desirable properties in discrete-time variable structure control (DVSC) (Yu, Chang, and Shi, 1996), (Xia, et al., 2010), (Corradini, et al., 2012). A decoupled disturbance compensator (DDC) with DVSC was proposed (Eun, et al., 1999), and for a faster response, a recursive switching function technique was also proposed (Kim, Oh, and Cho, 2000). Recently, a tuningless method for a servo drive based on the DVSC with DDC has also been developed (Bahn, et al., 2014). However, this method was limited to a motor with belt-drive load, which is not as harsh as a ball-screw load.

In this paper, a DVSC control method for a servo drive is developed and tested, using a 400 W servo motor with a belt-drive connection and a 400 W servo motor with a ball-screw connection. The feasibility of achieving tuningless control for the two different load types is shown.

2. CONVENTIONAL CONTROLLER STRUCTURE

Figure 1 shows a commercial PID-based servo drive structure under investigation in this paper. The dotted part is implemented on a digital signal processing (DSP) chip and application specific integrated circuit (ASIC). The control structure consists of two main loops, a position control loop and a velocity control loop. The controllers in these loops are PI controllers. Tunable digital filters, such as low-pass filters and notch filters, are also used to improve the stability of this system. A feedforward controller is also used to shorten the response time. This conventional structure can be very effective, but the gain-tuning process takes much time and does not perform well when load conditions are changed.

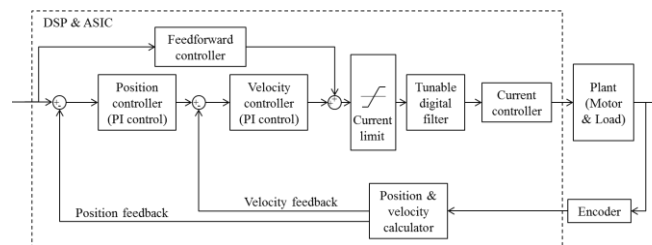


Fig. 1. Servo controller structure under investigation in this paper

3. DVSC METHOD FOR TUNINGLESS CONTROL

Figure 2 represents the block diagram of the developed tuningless servo control method. This control system has one

control loop, which utilizes the recursive DVSC (RDVSC) with DDC.

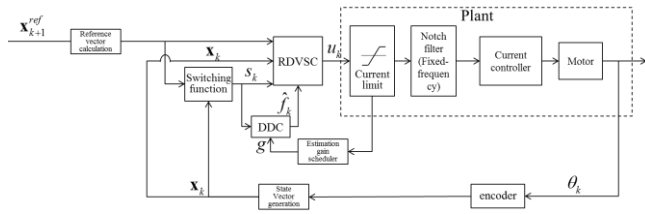


Fig. 2. Tuningless RDVSC+DDC servo drive control structure

A discrete SISO LTI system described:

$$\mathbf{x}_{k+1} = \Phi \mathbf{x}_k + \Gamma u_k \quad (1)$$

Considering parametric uncertainties and a disturbance, the system (1) is redefined as follows:

$$\mathbf{x}_{k+1} = (\Phi + \Delta\Phi) \mathbf{x}_k + (\Gamma + \Delta\Gamma) u_k + \mathbf{d}_k \quad (2)$$

where $\mathbf{x}_k \in \mathbf{R}^{n \times 1}$ is a state vector of sampling instant k , $u_k \in \mathbf{R}^1$ is an input, $\mathbf{d}_k \in \mathbf{R}^{n \times 1}$ is an external disturbance vector, $\Delta\Phi$ and $\Delta\Gamma$ are parametric uncertainties and control gain uncertainties, respectively. If there exist an $1 \times n$ row vector $\bar{\mathbf{a}}$, a scalar \bar{b} , and a scalar \bar{d}_k , which hold $\Delta\Phi = \Phi \bar{\mathbf{a}}$, $\Delta\Gamma = \Gamma \bar{b}$, $\mathbf{d}_k = \Gamma \bar{d}_k$. Then it is possible to rewrite the system (2) as follows:

$$\mathbf{x}_{k+1} = \Phi \mathbf{x}_k + \Gamma u_k + \Gamma h_k \quad (3)$$

where $h_k = \bar{\mathbf{a}} \mathbf{x}_k + \bar{b} u_k + \bar{d}_k$ is a generalized disturbance. For the generalized system (3), the RDVSC with DDC method were proposed earlier (Eun, et al., 1999), (Kim, Oh, and Cho, 2000), and applied to a belt-drive servo system (Bahn, et al., 2014). This paper presents more general cases including a ball-screw connection and more detailed experimental results.

For a servo drive, the state vector \mathbf{x}_k consists of the angle and angular velocity of a motor. The reference vector \mathbf{x}_k^{ref} also has the same form.

$$\mathbf{x}_k = \begin{bmatrix} \theta \\ \omega \end{bmatrix} \quad (4)$$

A switching function is defined using an error vector $\mathbf{e}_k = \mathbf{x}_k - \mathbf{x}_k^{ref}$ and an $1 \times n$ row vector G as follows:

$$s_k = G \mathbf{e}_k + \gamma s_{k-1}. \quad (5)$$

A control input is determined using the switching function is described:

$$u_k = -\hat{h}_k + (G\Gamma)^{-1} \left[-G\Phi \mathbf{x}_k + G\mathbf{x}_{k+1}^{ref} - \gamma s_k + q s_k - \eta \text{sat} \left(\frac{s_k}{\phi} \right) \right] \quad (6)$$

where q is asymptotic convergence rate, η is robustness parameter, and $\phi > 0$ is a boundary layer thickness. The saturation function is:

$$\text{sat} \left(\frac{s_k}{\phi} \right) = \begin{cases} \text{sgn}(s_k) & \text{if } |s_k| > \phi, \\ \frac{s_k}{\phi} & \text{if } |s_k| \leq \phi. \end{cases} \quad (7)$$

The estimated generalized disturbance, \hat{h}_k , is given as follows:

$$\hat{h}_{k+1} = \hat{h}_k + (G\Gamma)^{-1} g \left[s_k - q s_{k-1} + \eta \text{sat} \left(\frac{s_{k-1}}{\phi} \right) \right] \quad (8)$$

where a scalar g is the gain of the disturbance estimation updates. This estimation structure can suffer from an over estimation problem when the current output saturates. Thus, an estimation gain scheduler is designed to prevent the over estimation as follows:

$$g = \begin{cases} g_{normal} & \text{if } \text{abs}(u_k) < i_{lim}, \\ 0 & \text{if } \text{abs}(u_k) > i_{lim}. \end{cases} \quad (9)$$

4. EXPERIMENTS AND RESULTS

In this paper, a Tamagawa 400 W motor is used for experiments. A load can be connected either by a belt-drive or a screw-drive. In either case, the nominal continuous plant model of a servo motor is:

$$\dot{\mathbf{x}} = A\mathbf{x} + B u \quad (10)$$

where $A = [0, 1; 0, 0]$, $B = [0, k_t / J]^T$, and J is the inertia of the nominal plant model, and k_t is a torque constant. These parameters can be determined by the physical parameters of the motor. For the Tamagawa 400 W motor, the rotor inertia is $0.34 \text{ kg}\cdot\text{cm}^2$ and k_t is $0.2756 \text{ N}\cdot\text{m}/\text{A}$. In this paper, the selected nominal load inertia is 5 times to the rotor inertia, i.e., J is $1.70 \text{ kg}\cdot\text{cm}^2$.

Using the Tustin approximation, the continuous model is transformed to the discrete form. The sampling time of the control loop is $200 \mu\text{s}$. The discrete system model for the 400 W motor is:

$$\mathbf{x}_{k+1} = \Phi \mathbf{x}_k + \Gamma u_k \quad (11)$$

$$\text{where } \Phi = \begin{bmatrix} 1 & 2.0e-4 \\ 0 & 1 \end{bmatrix}, \Gamma = \begin{bmatrix} 3.292e-5 \\ 0.329 \end{bmatrix}.$$

Two different types of load, a belt-drive and a ball-screw are used for the experiments. The ball-screw is much stiffer than the belt-drive. In the experiments, the RDVSC control parameters are differently applied to the each case. Table 1 shows the selected control parameters.

Table 1. Selected parameters

Parameter	G	q	η	φ	g	γ
Belt-drive	[100 1]	0.95	5	50	0.05	0.001
Ball-screw	[100 1]	0.95	0.5	50	0.05	0.001

The experimental environments is shown in Fig. 3. There are two 400 W Tamagawa servo motors, which are connected to either a belt-drive load or a ball-screw load. A 17-bit encoder is integrated with the motor. The developed controller and the conventional controller are both implemented on the servo drive, and each control method is separately evaluated for comparison.

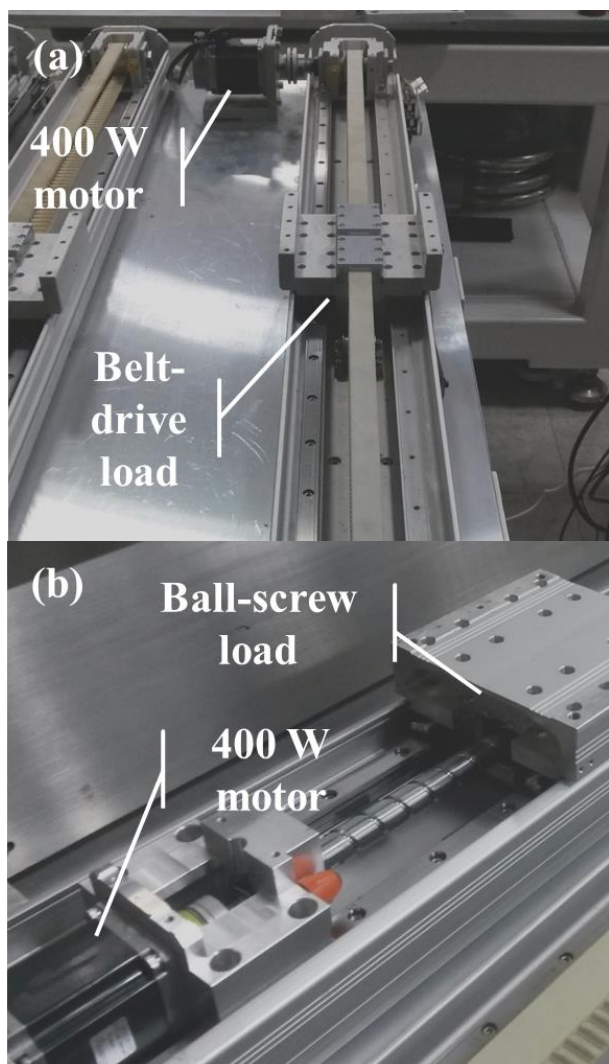


Fig. 3. Experimental environments
(a) Belt-drive
(b) Ball-screw

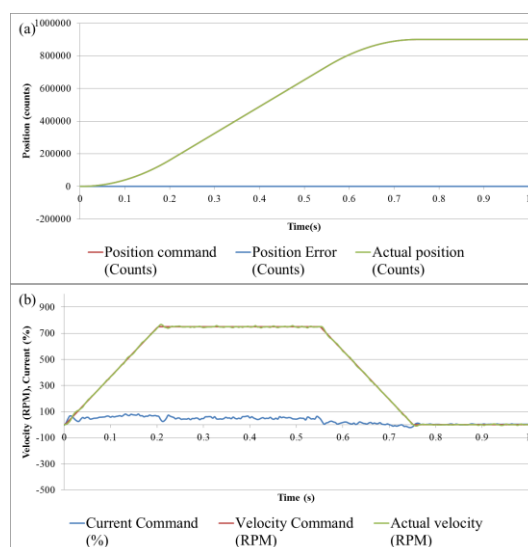
The evaluation methods are identical for every experiments. The reference commands are predetermined by the trajectory parameters: the target distance is 7 revolutions of the motor (i.e., 917,504 counts), the maximum velocity is 750 rpm, and the acceleration and deceleration times are both 200 ms. The tack time is used to quantify the performance. The tack time is defined as the time interval between the points that the commands and the actual values of position reach the target. In this paper, the start point of the measuring the tack time is when the position command trajectory reaches the target, and the end point is when the position error value reduces to within 10 counts (for a 17-bit encoder, 0.27°).

For both belt-drive and screw-drive load cases, two different controllers, i.e. the developed controller and the conventional controller, are evaluated. The developed controller has the control parameters of Table 1. The parameters of the conventional controller are manually tuned by an expert for each type of load with no additional weight to a level similar to an actual field implementation.

The experimental results using the belt-drive are shown in Figs. 4-7 and summarized in Table 2. For the belt-drive with no additional weight, the load inertia is 22.79 times larger than rotor inertia of the motor. The tack time performance of the developed method is 34 ms, which is similar to that of the conventional method, 32 ms. With an additional weight of +2 kg, the tack time of the developed method is 77 ms, which compares well to the 98 ms in the conventional method.

Table 2. Summary of belt-drive experiments

Experiment conditions		Performance (tack time)	
Types of motor & load	Additional weight (Total load ratio to rotor)	Proposed method	Conventional method
400W motor, Belt-drive load	+0 kg (22.79)	34 ms	32 ms
	+2 kg (45.77)	77 ms	98 ms



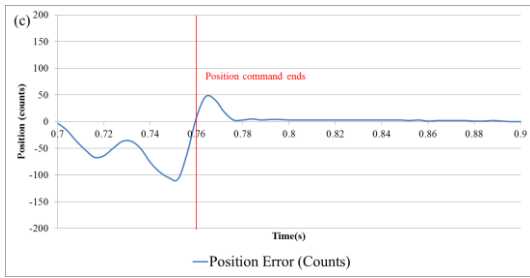


Fig. 4. Experiment results of the proposed controller (load type: belt-drive, load inertia: 22.79)
(a) Position command, position error, and actual position
(b) Current command, velocity command, and actual velocity
(c) Position error (enlarged)

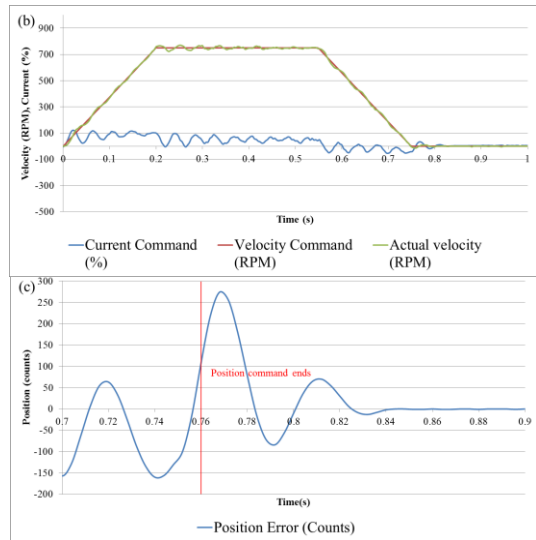


Fig. 6. Experiment results of the proposed controller (load type: belt-drive, load inertia: 45.77)
(a) Position command, position error, and actual position
(b) Current command, velocity command, and actual velocity
(c) Position error (enlarged)

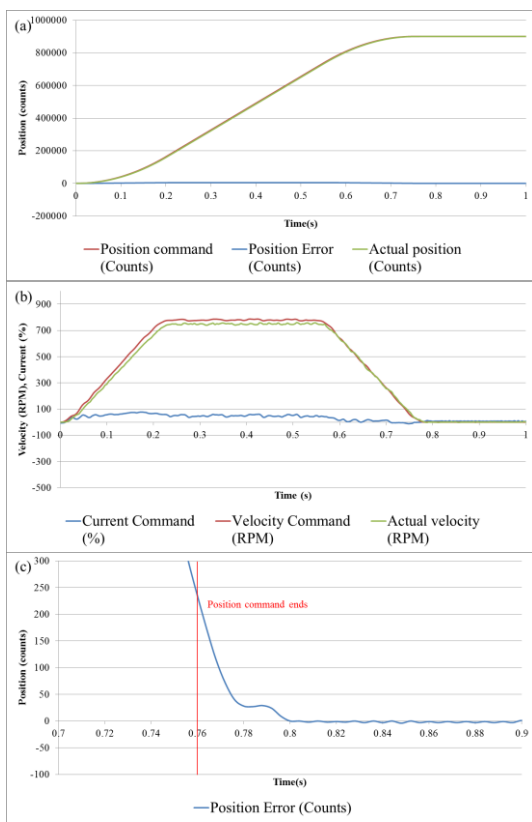


Fig. 5. Experiment results of the conventional method (load type: belt-drive, load inertia: 22.79)
(a) Position command, position error, and actual position
(b) Current command, velocity command, and actual velocity
(c) Position error (enlarged)

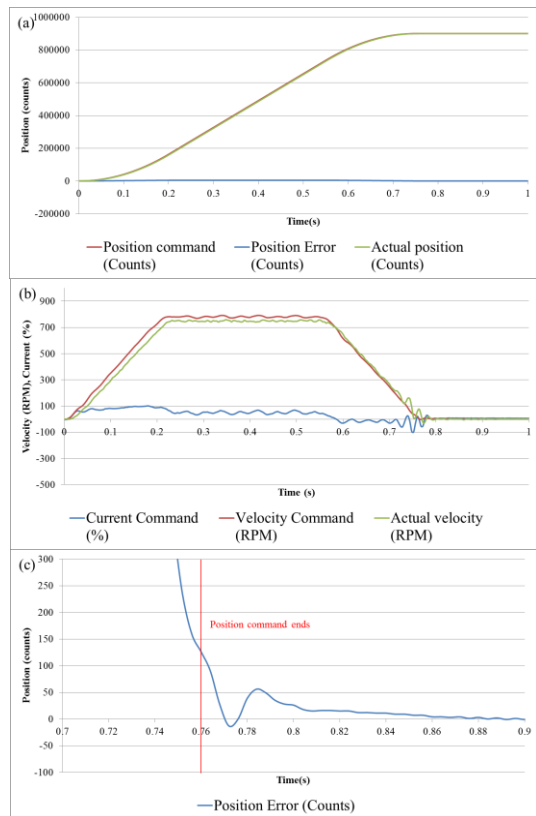
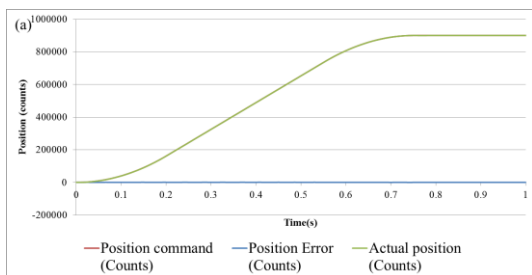


Fig. 7. Experiment results of the conventional method (load type: belt-drive, load inertia: 45.77)
(a) Position command, position error, and actual position
(b) Current command, velocity command, and actual velocity
(c) Position error (enlarged)



The experimental results using the ball-screw are shown in Figs. 8-11 and summarized in Table 3. For the ball-screw

with no additional weight, the load inertia is 5.79 times larger than rotor inertia of the motor. With no additional weight, the tack time performance of the developed method is 42 ms, which is similar to that of the conventional method, 40 ms. However, when the load weight gets heavier, the performance of the conventional method gets worse: 41 ms with an additional weight of +5 kg, 56 ms with an additional weight of +10 kg, and 92 ms with an additional weight of +15 kg. On the other hand, the tack performance of the developed controller is maintained even if the load weight varies: 41 ms with an additional weight of +5 kg, 40 ms with an additional weight of +10 kg, and 36 ms with an additional weight of +15 kg.

Table 3. Summary of ball-screw experiments

Experiment conditions		Performance (tack time)	
Types of motor & load	Additional weight (Total load ratio to rotor)	Proposed method	Conventional method
400W motor, Ball-screw load	+0 kg (5.79)	42 ms	40 ms
	+5 kg (7.40)	41 ms	41 ms
	+10 kg (8.84)	40 ms	56 ms
	+15 kg (10.37)	36 ms	92 ms

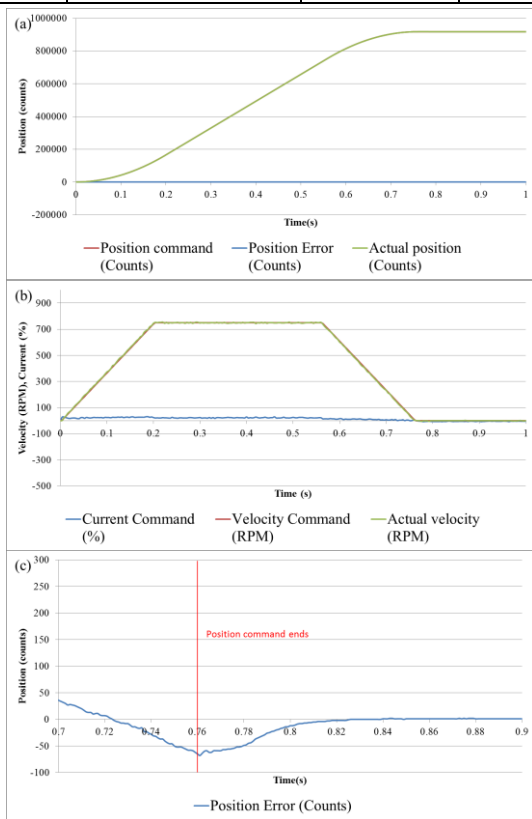


Fig. 8. Experiment results of the proposed controller (load type: ball-screw, load inertia: 5.79)
 (a) Position command, position error, and actual position
 (b) Current command, velocity command, and actual velocity
 (c) Position error (enlarged)

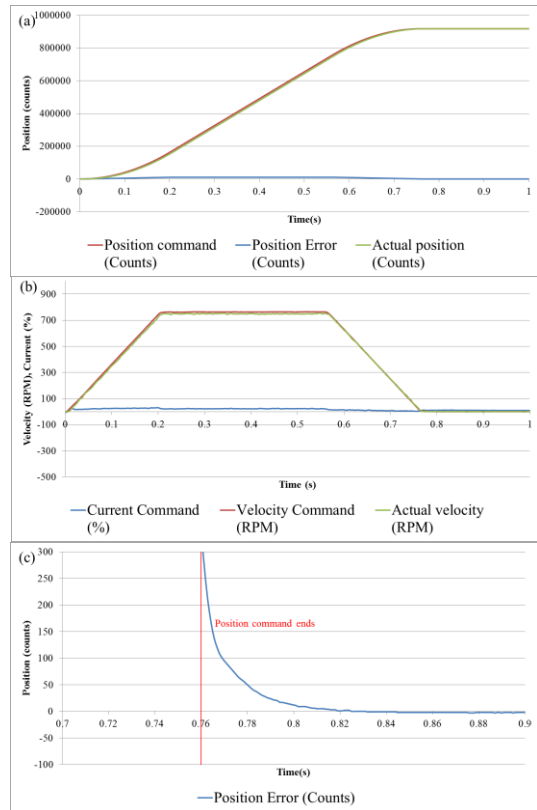


Fig. 9. Experiment results of the conventional method (load type: ball-screw, load inertia: 5.79)
 (a) Position command, position error, and actual position
 (b) Current command, velocity command, and actual velocity
 (c) Position error (enlarged)

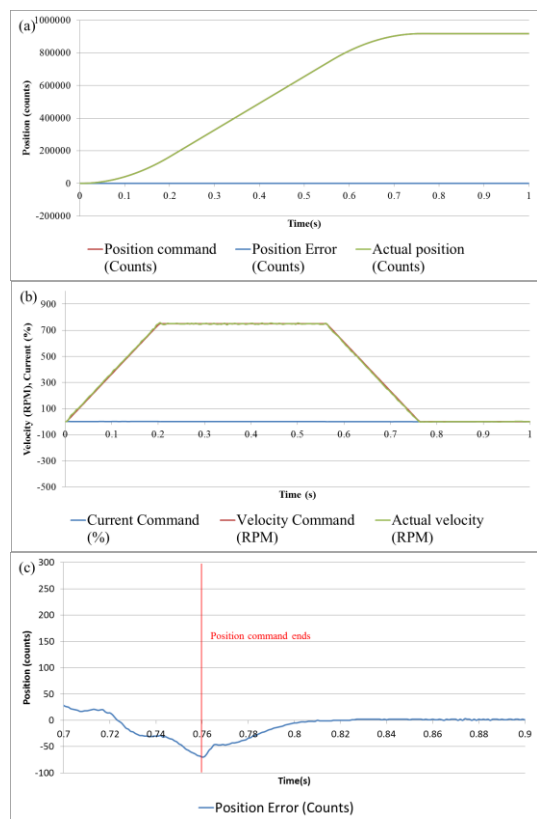


Fig. 10. Experiment results of the proposed controller (load type: ball-screw, load inertia: 10.37)
(a) Position command, position error, and actual position
(b) Current command, velocity command, and actual velocity
(c) Position error (enlarged)

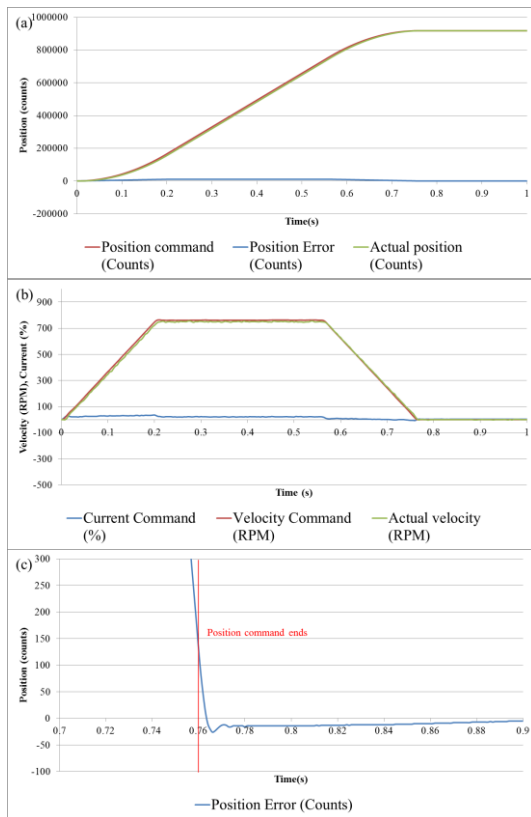


Fig. 11. Experiment results of the conventional method (load type: ball-screw, load inertia: 10.37)
(a) Position command, position error, and actual position
(b) Current command, velocity command, and actual velocity
(c) Position error (enlarged)

5. CONCLUSIONS

A RDVSC control method for a servo drive is developed. The performance of the developed control method is evaluated using a 400 W servo motor with two different type of load, a belt-drive load and a ball-screw. A conventional PI-based servo drive controller, which is manually tuned for a level similar to an actual field implementation, is also evaluated to compare with the developed method. The condition for manual tuning for the belt-drive is that the inertia of the load is 22.79 times larger than that of the rotor. With no additional weight, the tack time performances of the developed and conventional methods are similar, 34 ms to 32 ms, respectively. However, with an additional weight of +2 kg, load inertia becomes 45.77 times larger than that of the rotor, the developed controller has better tack time performance than that of the conventional controller, specifically 77 ms to 98 ms. For the ball-screw load with no additional weight, the load inertia is 5.79 times larger than that of the rotor. With no additional weight, the tack time performances of the developed and conventional methods are similar, 42 ms to 40 ms, respectively. However, when the

load weight gets heavier, the tack time performances of the developed method are better than those of the conventional method: 41 ms to 41 ms for + 5 kg, 40 ms to 56 ms for + 10 kg, and 36 ms to 92 ms for +15 kg. Based on these results, the developed method provides better performance for a wide range of load conditions for the tuningless control of servo systems.

ACKNOWLEDGEMENT

This work was supported by the R&D program of Korea Ministry of Trade, Industry and Energy (MOTIE) [10045630, Development of tuningless, high-performance servo system series with functional safety].

REFERENCES

- Bahn, W., Lee, S., Lee, S., and Cho, D. (2014). Tuningless Servo Controller Using Variable Structure Control and Disturbance Compensation. *Proceedings of ICIT Conference*, 96-99.
- Corradini, M. L., Fossi, V., Giantomassi, A., Ippoliti, G., Longhi, S., and Orlando, G. (2012). Discrete time sliding mode control of robotic manipulators: Development and experimental validation. *Control Engineering Practice*, 20 (8), 816-822.
- Eun, Y., Kim, J., Kim, K., and Cho, D. (1999). Discrete-time Variable Structure Controller with a Decoupled Disturbance Compensator and Its Application to a CNC Servomechanism. *IEEE Transactions on Control System*, 4, pp. 414-423.
- Gao, W., Wang, Y., and Homaifa, A. (1995) Discrete-time variable structure control systems. *IEEE Transactions on Industry Electronics*, 42 (2), 117-122.
- Hung, J. Y., Gao, W., and Hung, J. C. (1993). Variable structure control: A survey. *IEEE Transactions on Industry Electronics*, 40 (1), 2-22.
- Kim, J., Oh, S., and Cho, D. (2000). Robust Discrete-Time Variable Structure Control Methods. *Journal of Dynamic Systems*, 122 (2) 766-775.
- Leonhard, W. (2001). *Control of Electrical Drives*, Springer-Verlag.
- Xia, Y., Zhu, Z., Li, C., Yang, H., and Zhu, Q. (2010). Robust adaptive sliding mode control for uncertain discrete-time systems with time delay. *Journal of the Franklin Institute*, 347 (1), 339-357.
- Yu, F., Chang, Z. X., and Shi, Y. W. (1996). Variable structure control of discrete-time systems and their quality. *Proceedings of ICIT Conference*, 816-820.